Acta of Bioengineering and Biomechanics
Vol. 11, No. 2, 2009

Original paper

Multiscale FEM model of artificial heart chamber composed of nanocoatings

ANDRZEJ MILENIN*, MAGDALENA KOPERNIK

Department of Applied Computer Science and Modelling,
AGH University of Science and Technology, Kraków, Poland.

The purpose of the present work was to construct the multiscale FEM model of artificial heart chamber composed of nanocoatings. This goal is reached by the development of the FEM macromodel of artificial blood chamber using the commercial code and by the creation of the micromodel based on our own FEM code. The latter uses strain state obtained after loading in macromodel. The loci of failure initiation in the material of chamber were precisely determined and these results are used as an input data for the new micromodel.

Key words: *multiscale model, finite element method (FEM), heart chamber, nanocoating, representative volume element (RVE)*

1. Introduction

The heart is composed of two chambers: the right-side chamber supplying the lungs and the left one pumping oxygenated blood through the body. The chambers, particularly the left one, are prone to diseases and may have to be replaced. In the case of irreversible and degenerative failure, the human heart chamber cannot work properly and must be temporarily or permanently replaced with prosthesis – artificial heart chamber [1]. Polyurethane (PU) is intended to be used as a construction material of the artificial blood chamber. It has been found that the blood clot formation proceeds in the polyurethane/blood contact area and the polyurethane is subjected to degradation. Therefore, there is a necessity to modify the surface of polyurethane by covering it with a biocompatible coating. TiN deposited by PLD (Pulsed Laser Deposition) method is supposed to improve not only the material properties of coated specimen, but also its biocompatibility [2]. The main advantage of using the PLD method is low temperature of the deposition process (room temperature), which does not change the properties of the substrate. This method has the disadvantage that TiN coatings are deposited on polyurethane surface at the high values of compressive stresses in TiN coatings (residual stress equals about 10 GPa) because of the character of surface modification process. Therefore, in the future model of chamber, the distribution of residual stresses, which are experimentally examined after the deposition process in coatings, should be considered. This leads to a high risk of degenerative failure of these coatings, especially in the region of polyurethane/TiN contact. The stress concentration in coating and in the area of coating/PU contact is thought to be one of the main reasons responsible for degeneration of the heart chamber composed of PU/TiN. Making this assumption it is possible to evaluate the influence of outer coating on fracture probability in the model of chamber by applying the multiscale approach.

* Corresponding author: Andrzej Milenin, Department of Applied Computer Science and Modelling, Faculty of Metals Engineering and Industrial Computer Science, AGH University of Science and Technology, al. Mickiewicza 30, 30-059 Kraków, Poland. E-mail: milenin@agh.edu.pl

Received: January 28th, 2009
Accepted for publication: April 22nd, 2009

Because of the above, our aim was to evaluate the outer coating deposited on polyurethane of artificial blood chamber, especially to calculate the values of strain and stress, and further to estimate as precisely as the probability of irreversible fracture on the basis of microscale model. Since the testing of a whole multilayered model of artificial heart chamber would be time-consuming, the multiscale FEM approach is adopted and applied only locally in this area of the model, which seems to be most liable to suffer fracture under the predicted and modelled loadings. Thus, the prediction of stress and strain distributions under loading is helpful in designing the shape and selecting the coatings for heart chamber.

2. Macroscale model of artificial heart chamber and its limitations

The physical model of artificial blood chamber connected to the model of man is shown in figure 1. The shape of the artificial chamber during filling phase and its main parts are given in figure 2. The geometry of this chamber in its final version (figure 3) was based on CAD program being used in the FEM model. The geometrical model of artificial left blood chamber was fully prepared by the LITWIŃSKI et al. [1] who form the research group in the Foundation of Cardiac Surgery Development in Zabrze (FRK) founded by Professor Z. Religa. The full physical model of artificial heart is composed of two connectors (inlet and outlet), the biggest part – blood bowl, the large but simultaneously very thin pneumatic bowl and two valves (inlet and outlet mechanical valves, commercial Medtronic, Moll, or three-leaflet polyurethane valve). The geometry of the chamber applied in the present paper is slightly simplified. The modifications introduced into the chamber model lead to shortening the connectors by cutting at these cross sections where valves are located. This reduced model of chamber was prepared by the authors of present work in Solid Works program. The processing of our model of chamber leads not only to the modification of its final geometry, but also to the meaningful improvement of this geometry quality. All the geometry defects noticed were eliminated by the authors of the present work. A good quality of technical drawing imported into FEM program is required because of the necessity of mesh generation. It is impossible to obtain fine mesh based on the geometry, whose lines are open or crossed. At first sight, the model of chamber seems very simple, but in fact it is very difficult to reproduce its precise geometry by using standard CAD programs and therefore many errors occur in the geometry. Our final model of the chamber geometry (based on FRK full model) is composed of two main parts: the top pneumatic bowl and the bottom blood bowl as well as two channels: reduced connectors. After repairing procedures the prepared model of geometry is written into all available Solid Works formats, which are imported by ABAQUS, ADINA and other commercial FEM programs.

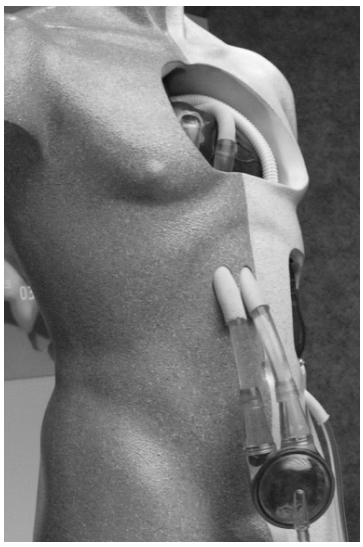

Fig. 1. Physical model of artificial blood chamber POLVAD connected to the model of man [1]

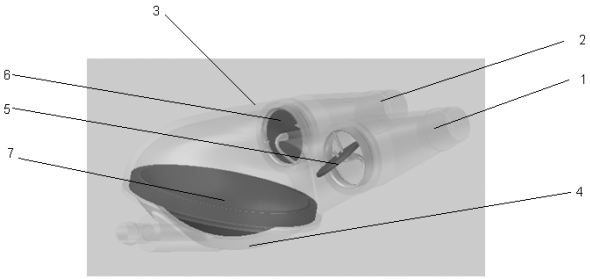

Fig. 2. Scheme of artificial heart chamber POLVAD: 1 – inlet connector, 2 – outlet connector, 3 – blood bowl, 4 – pneumatic bowl, 5 – inlet valve, 6 – outlet valve, 7 – membrane in filling phase [1]

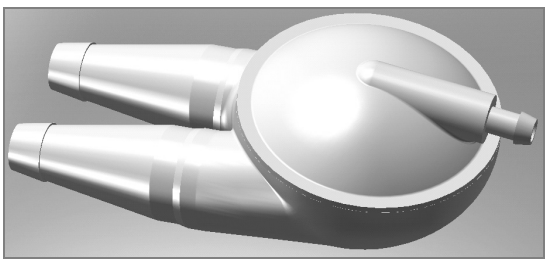

Fig. 3. Geometry of artificial heart chamber POLVAD

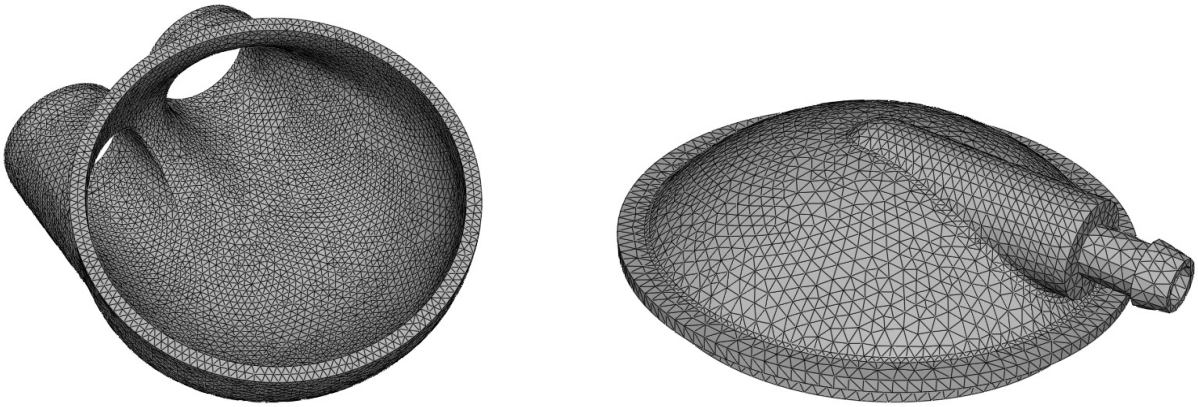

a) b)

Fig. 4. Bottom (a) and top (b) parts of FEM model of chamber

The whole 3D FEM model of the chamber was performed in ABAQUS. FEM models of chamber elements are presented in figure 4. 21339 and 7572 node finite elements are used to solve the boundary problem for the cases in figure 4a and figure 4b, respectively. Average computing time of each simulation is about 15 minutes. A static loading uniformly set to inner surface of the model is equal to 16 kPa, which is the maximum physiological blood pressure observed in the left heart chamber. The model proposed has some limitations and one of them is arriving at the solution without FSI (fluid structure interaction) approach. From our point of view the model under analysis is not sensitive enough to mechanical reaction of blood chamber wall to fluid flow. The interactions between these two media can be neglected compared with those observed in blood flow. The explanation of our reasoning is very simple and based on the Newtonian mechanics. The predicted acceleration of the points of chamber is assumed to be very small (approaching zero). Therefore, small forces of inertia are registered. Their values are very small in comparison with the forces observed in blood flow. Therefore, in our model of chamber, the dynamics of the mechanical model is omitted and only static loading is set to the inner surface of the object analysed.

In macroscale model, the basic chamber material, i.e. polyurethane (Chronothane 55D), is assumed to be purely elastic and characterised by Young's modulus $E = 423$ MPa and the Poisson ratio $\nu = 0.4$. Because of this fact, the values of elastic properties limited by Young's modulus are high and the stiffness of construction material (polyurethane) is also quite high. This allows us to expect small values of computed stress and strain in the model examined under the predicted and set values of real loading (maximum pressure of blood in left chamber), which is also investigated in the present work. Because of the introduced input values of properties the model of chamber is not susceptible to severe deformations and displacements, which additionally confirms that the limitations of the model applied and considered here as static loading are acceptable.

Our macromodel is based only on the material of which the linear elastic model is made. Assuming the linear elasticity of materials is a simplification, because the real material model of polyurethane is nonlinearly elastic and TiN is an elastoplastic material. On the basis of our coworkers knowledge (the other performers of Polish Artificial Heart Project, especially research group in FRK) it is impossible to reach the stress values in the walls of chamber (under expected loading, i.e. the pressure in the left chamber of heart), which are higher than those of stress reached in linearly elastic range measured for polyurethane and TiN. Another assumption consulted with coworkers specialized in material science is that the stresses are not the function of velocity in the ranges of values reached in the chamber walls. Therefore, the simplification of material models is really advantageous, since it limits the computing time and does not introduce the error caused by a wrong assumption for type of material models.

3. Microscale model of artificial heart chamber

The analysis of strain distributions at the inner surface of heart chamber in the macroscale FEM model is helpful in determining correctly the areas in which is the highest probability that failure will oc-

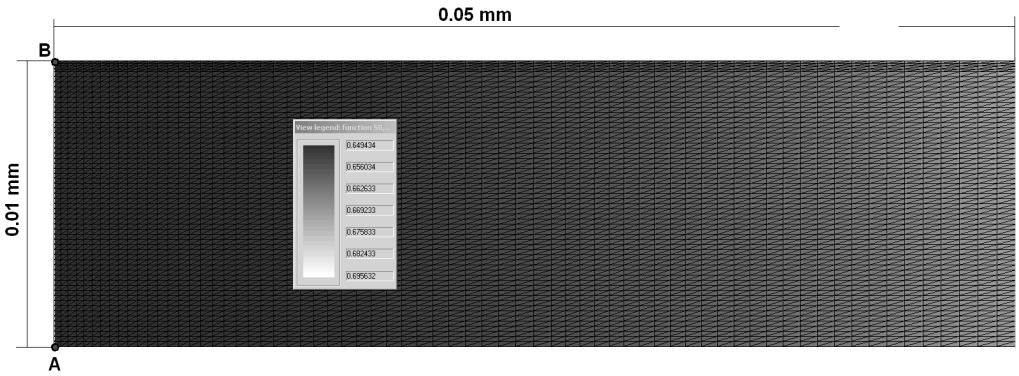

Fig. 5. Dimensions of representative volume element and distribution of average stress in material of artificial heart chamber made of PU

cur. Therefore, only these places are further taken into account and investigated in the microscale model. Subsequently, the strain state reached during loading in macromodel is introduced into FEM micromodel. The representative volume element (RVE) shown in figure 5 is composed of substrate (polyurethane) material layer coated with a very thin TiN layer, whose thickness is expressed in nanometers (it is assumed to be 40 nm in the present test). Additionally, the example of the distribution of the average stress computed for model composed only of PU is shown in figure 5.

A 2D FEM micromodel of failure initiation in the part of the chamber implemented in authors' FE code has 4-node finite elements, which are used to solve the boundary problem. The developed FE model of the RVE is composed of 5162 elements, 5310 nodes and an average computing time of each simulation is about 5 min on standard PC.

The material model of TiN was identified in earlier papers [3], [4], [6] using the 2D FEM model of the system of coatings prepared in the FE code. Inverse analysis described in [5] was applied to determine the mechanical properties of TiN coating. In the present paper, the material model of a thin TiN coating is assumed to be purely elastically defined by Young's modulus E = 20 GPa and the Poisson ratio ν = 0.177, because from designer's point of view the plastic deformation of the material model of the outer coating of heart chamber is not allowed. We observed the inhomogeneity of mechanical properties between TiN coating and polyurethane. Thus, it is fustified to assume the elastoplastic or non-linear elastic material model. In consequence, the boundary problem in the FEM micromodel is solved considering the following phenomena: elastic as well as elastoplastic deformation and unloading process (in the elastoplastic case).

The elastic and elastoplastic theory is used to arrive at the solution for the defined boundary problem. On the basis of this theory, the stress field is calculated directly using the strain fields and the relations listed below:

(i) differential equations of equilibrium:

$$\sigma_{ij,j} = 0\,; \tag{1}$$

(ii) differential equations of the connection between displacements and strains:

$$\varepsilon_{ij} = \frac{1}{2}(u_{i,j} + u_{j,i})\,; \tag{2}$$

(iii) relation between stresses and strains:

$$\sigma_{ij} = \delta_{ij} k \varepsilon_0 + \frac{3\sigma_i}{2\varepsilon_i}(\varepsilon_{ij} - \delta_{ij}\varepsilon_0)\,, \tag{3}$$

where: σ_{ij} – the stress tensor, ε_{ij} – the strain tensor, u – the displacement vector, $k = \dfrac{E}{1-2\nu}$ – the coefficient of volumetric strain, ε_0 – the volumetric strain, ν – Poisson's ratio, the Kronecker symbol:

$$\delta_{ij} = \begin{Bmatrix} 1 & \text{if} & i = j \\ 0 & \text{if} & i \neq j \end{Bmatrix},$$

ε_i – the effective strain and σ_i – the effective stress (is equal to flow stress in plastic zone).

Equation (2) describes geometrical properties of elastic bodies. In the case of elastoplastic bodies, the form of this equation is very simplified because the nonlinear terms are omitted. Equation (3) can be applied but it is a simplified form, because the second term does not satisfy the laws of material conditions in the aspect of theoretical mechanics.

The boundary conditions are modelled according to the following principles. The deformation tensor (ε_1, ε_2, ε_3) is obtained from the macromodel. The value of the strain ε_2 is introduced into the micromodel as a constant. Therefore, the 3D boundary problem of RVE deformation is transformed into the 2D plane strain problem with the present value of ε_2. The principles for ε_1 and ε_3 are also used in the micromodel of the RVE.

The standard FEM approach is applied to the nonlinear elastic problems, and the non-elastic theory is used [7]; on the basis of the known variational principle we obtain the functional form expressed by the following equation:

$$J = \int_V \left(\int_0^{\varepsilon_i} \sigma_i d\varepsilon_i \right) dV + \int_V k\varepsilon_0^2 dV - \int_S p_n u_n dS, \quad (4)$$

where: V – the volume of the domain, S – the contact surface, p_n – the pressure directed perpendicularly to the contact surface, u_n – the normal displacement.

The results of using equation (4) are the solution and the stiffness matrix. The general form of equation (4) after substituting the real effective stress function (flow stress) for the materials under analysis (polyurethane and TiN) leads to a nonlinear form of equation (4). That is why it needs linearization. As long as the function used for effective stress (flow stress) is nonlinear it needs to increase monotonically (it cannot decrease). The linearization is practically performed by introducing the elastoplastic modulus, called the effective Young's modulus E'. E' is defined by the relation between the flow stress and the effective strain as follows:

$$E' = \frac{\sigma_i(\varepsilon_i)}{\varepsilon_i}. \quad (5)$$

The described linearization procedure of this functional form explained in [3] leads to the simplified formula:

$$J = \int_V E'\varepsilon_i^2 dV + \int_V k\varepsilon_0^2 dV - \int_S p_n u_n dS, \quad (6)$$

where E' is effective Young's modulus equal to Young's modulus in elastic zone.

In order to model the unloading step in the case of elastoplastic deformation, one relies on the theorem of unloading introduced in [7]. According to this theorem the following algorithm is performed during every time step of unloading:

(i) The fields of stress σ_{ij} and strain ε_{ij} before unloading are the solutions of the problem for active loading.

(ii) Then the specimen is loaded with the inverse force and the material is modelled as elastic. After this procedure the fields of σ_{ij}^e and ε_{ij}^e are obtained.

(iii) The actual state of stress and strain during the unloading stage is reached as the sum of the following solutions:

$$\sigma_{ij}^{\text{unload}} = \sigma_{ij} + \sigma_{ij}^e,$$
$$\varepsilon_{ij}^{\text{unload}} = \varepsilon_{ij} + \varepsilon_{ij}^e. \quad (7)$$

4. Macromodel results

The macromodel results are shown in figures 6–10. Figures 6 and 7 present the distributions of the average stress at the inner surface of the bottom and top parts of chamber in top and side views of cross-sections. Figures 8 and 9 show the distributions of the average stress at the inner surface of the top parts of chamber in top and side views of cross-sections.

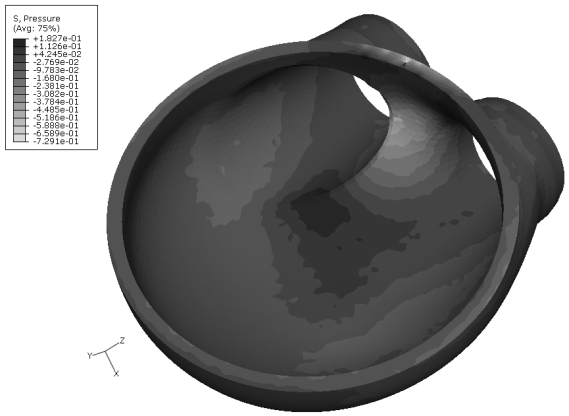

Fig. 6. Distributions of average stress at inner surface of bottom part of chamber (top view of cross-section)

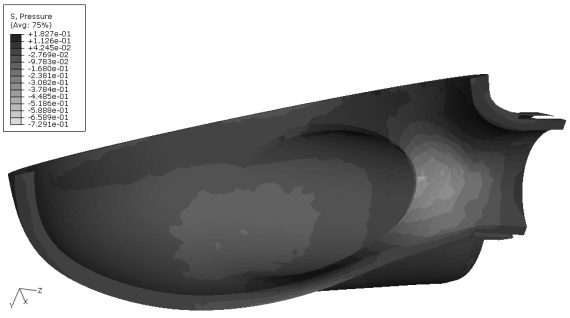

Fig. 7. Distributions of average stress at inner surface of bottom part of chamber (side view of cross-section)

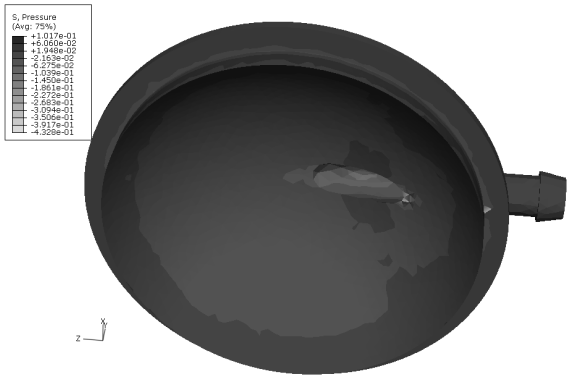

Fig. 8. Distributions of average stress at inner surface of top part of chamber (top view of cross-section)

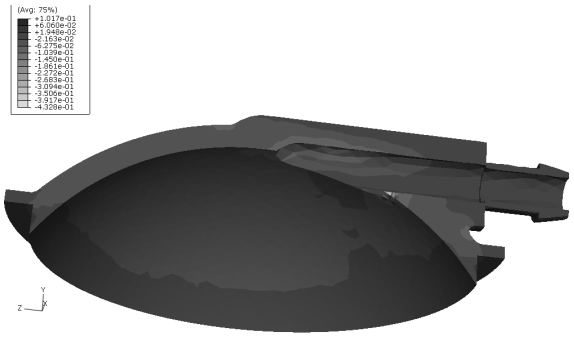

Fig. 9. Distributions of average stress at inner surface of top part of chamber (side view of cross-section)

The analysis of the results presented is helpful in locating the dangerous areas, where the values of average stress and strain are the highest. The principal strain ε_1 distribution is shown in figure 10. The critical region determined after the analysis of stresses and strains is indicated by the circle in this figure. The most degenerative area of loaded chamber surface, where the highest values of calculated strains are observed, is found on the inner surface of the bottom part of chamber in side view of the cross-section between two connectors. Accordingly, the boundary conditions (ε_1, ε_2, ε_3) for micromodel are obtained in this region.

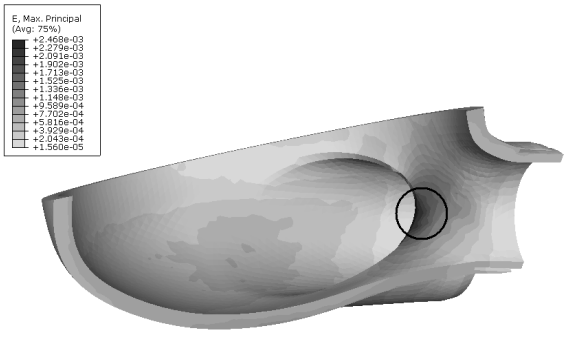

Fig. 10. Distributions of maximal principal strain ε_1 at inner surface of bottom part of chamber (side view of cross-section) and dangerous area

The numerical tests lead to the conclusion that the advantage of the chamber model performed lies in the fact that the highest values of stresses and strains have only local character. Thus, the probability of failure occurring is not the highest.

Additionally, the computed values of stress in the material of the chamber model do not exceed the linear elastic range measured for polyurethane. Therefore, this material of the chamber cannot be deformed nonlinearly and the use of nonlinear elastic material model is not valuable in the case examined.

5. Micromodel results

The micromodel results are presented in figures 11 and 12 as the distributions of Young's modulus, average stress and effective strain in representative volume element. The differences in the values of Young's modulus between adjacent layers considered as polyurethane and thin TiN coating are meaningful, which is confirmed by computed distributions. In the very thin region between two main material layers of TiN and PU, the effective strain has the highest value.

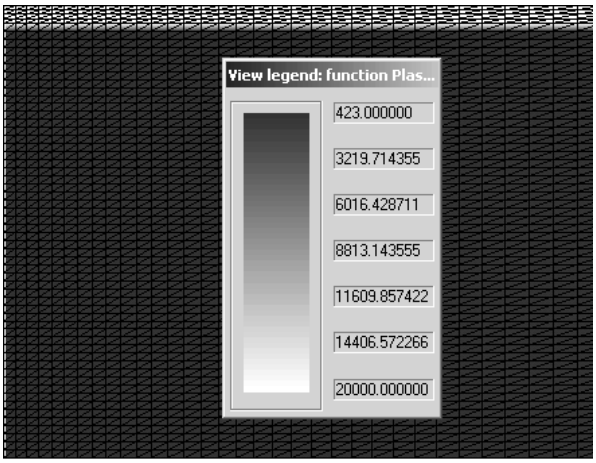

Fig. 11. Distribution of Young's modulus in representative volume element

The average stress in TiN layers (figure 12a) is equal to 20 MPa (0.7 MPa for PU chamber in figures 6 and 7). The computed values of stress in TiN and PU, the chamber model materials, do not exceed their linear elastic range measured experimentally. Therefore, the material of chamber cannot be nonlinearly deformed and the use of nonlinear elastic material model is not valuable in the case under examination.

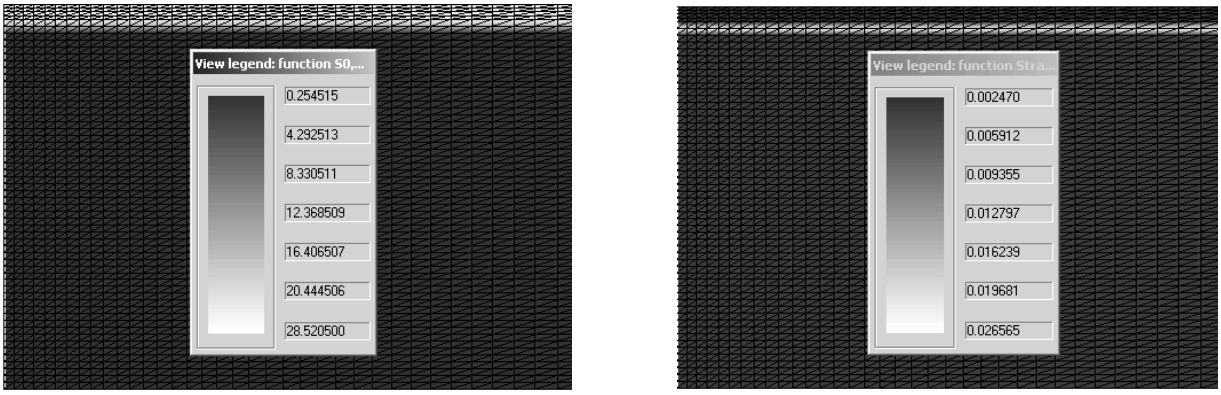

a) b)

Fig. 12. Distribution of average stress (a) and effective strain (b) in representative volume element

The highest values of the average stress and the effective strain in the boundary region between the two main material layers inclined us towards advanced lab experiments showing the connection quality during long-lasting work of the chamber. Therefore, it is necessary to run the unsteady dynamic simulation with physiological pressure variations over a full cardiac cycle of the microscale model of chamber materials, which should provide more faithful information about the long-term working of the chamber. This will be realized by implementing the complete material models of coating (elastoplastic material model) and substrate (PU – nonlinear elastic material model) because of fatigue investigations (shear stress analysis) of the chamber materials. The next and one of the most important research steps will be the introduction of the distribution of initial residual stresses into microscale FEM model of the chamber, which will be measured in the deposited TiN coatings.

6. Conclusions

The approach proposed in the present paper was adopted to construct the multiscale FEM model of artificial heart chamber composed of nanocoatings. The results obtained lead to the following conclusions:

1. The developed macroscale FEM model based on the commercial code ABAQUS is able to reproduce the strain and stress states in the material of the artificial blood chamber. The predicted distributions of selected parameters are helpful in a precise defining those regions of the chamber, which can be recognized as very sensitive to failure. These areas require an extended multiscale modelling. Additionally, the values of strain calculated after loading are the input data for the micromodel.

2. The micromodel based on our own FEM code is composed of main material layer and very thin outer coating. The distributions of stresses and strains allow us to determine precisely the critical values of strain, which can occur in the materials studied.

3. In the macromodel, the region being especially vulnerable to fracture is located at the inner surface of the bottom part of the artificial blood chamber between two connectors.

4. In the micromodel, the region being especially vulnerable to fracture is defined as the very thin region between two main material layers (TiN and PU) at the inner surface of the bottom part of the artificial blood chamber between two connectors.

5. The results of previous papers [3], [4], which identified the parameters of TiN material model, as well as the mathematical model of the system of coatings were used in the present paper. The mathematical model of the system of coatings was modified according to the settings and conditions required. The main changes occur in boundary conditions (lack of friction) and simplified material model (only its elastic part is considered).

6. The extension of the chamber model developed can lead to a more precise information about the chamber long-term working and will be realized by reducing the limitations of the model presented as well as by overcoming many problems which have not been solved yet. Therefore, the following steps will be made in the nearest future:

i) introducing the distribution of initial residual stresses into microscale FEM model of the chamber,

ii) carrying out an unsteady simulation with physiological pressure variations over a full cardiac cycle,

iii) implementing the complete material models of each material layer because of the fatigue investigations (shear stress analysis) of the chamber.

Acknowledgements

Financial assistance of the MNiSzW, project no. 08/WK/P02/0001/SPB-PSS/2008, is acknowledged. Calculations were made in ACK CYFRONET AGH. Calculation grant number MNiSW/IBM_BC_HS21/AGH/020/2008.

Literature

[1] LITWIŃSKI P., WOŹNIEWICZ B., RELIGA G., PASTUSZEK M., PARULSKI A., JASIŃSKA M., KOCAŃDA S., KUSTOSZ R., SIONDALSKI P., RELIGA Z., *Zastosowanie mechanicznego wspomagania krążenia sztucznymi komorami typu POLVAD w leczeniu wstrząsu kardiogennego na tle zapalenia mięśnia sercowego*, Kardiochir. Torakochir. Pol., 2005, 2/4, 33–40.

[2] MAJOR R., BONARSKI J., MORGIEL J., MAJOR B., CZARNOWSKA E., KUSTOSZ R., LACKNER J.M., WALDHAUSER W., *Elastic TiN coating deposited on polyurethane by pulsed laser*, Surface and Coatings Technology, 2006, 200, 6340–6345.

[3] KOPERNIK M., MILENIN A., *The sensitivity analysis of nanoindentation test for specimen composed of TiAlN and TiN using the mathematical model*, Steel Research International, Special Edition, Metal Forming Conference, 2008, 79/2, 555–562.

[4] KOPERNIK M., MILENIN A., *Analiza próby nanotwardości dla powłok wielowarstwowych za pomocą modelu matematycznego*, Proc. XV KomPlasTech, F. Grosman, M. Hyrcza-Michalska (eds.), Korbielów, 2008, 65–72.

[5] SZELIGA D., PIETRZYK M., *Testing of the inverse software for identification of rheological models of materials subjected to plastic deformation*, Archives of Civil and Mechanical Engineering, 2007, 7/1, 35–52.

[6] KOPERNIK M., SZELIGA D., *Modelling of nanomaterials – sensitivity analysis to determine the nanoindentation test parameters*, Computer Methods in Materials Science, 2007, 7/2, 255–261.

[7] ILUSHIN A., *Plastyczność*, AN ZSSR, Moscow, 1963.